1-1-2020

Evaluating techniques for mapping island vegetation from unmanned aerial vehicle (UAV) images: Pixel classification, visual interpretation and machine learning approaches

Sarah Hamylton
University of Wollongong, shamylto@uow.edu.au

Rowena H. Morris
University of Wollongong, rowenam@uow.edu.au

Rafael Cabral Carvalho
University of Wollongong, rafaelc@uow.edu.au

N Roder
University of Wollongong

P Barlow
University of Wollongong

See next page for additional authors

Publication Details Citation

Hamylton, S., Morris, R. H., Cabral Carvalho, R., Roder, N., Barlow, P., Mills, K., & Wang, L. (2020). Evaluating techniques for mapping island vegetation from unmanned aerial vehicle (UAV) images: Pixel classification, visual interpretation and machine learning approaches. Faculty of Science, Medicine and Health - Papers: Part B. Retrieved from https://ro.uow.edu.au/smhpapers1/1327

Evaluating techniques for mapping island vegetation from unmanned aerial vehicle (UAV) images: Pixel classification, visual interpretation and machine learning approaches

Abstract

We evaluate three approaches to mapping vegetation using images collected by an unmanned aerial vehicle (UAV) to monitor rehabilitation activities in the Five Islands Nature Reserve, Wollongong (Australia). Between April 2017 and July 2018, four aerial surveys of Big Island were undertaken to map changes to island vegetation following helicopter herbicide sprays to eradicate weeds, including the creeper Coastal Morning Glory (Ipomoea cairica) and Kikuyu Grass (Cenchrus clandestinus). The spraying was followed by a large scale planting campaign to introduce native plants, such as tussocks of Spiny-headed Mat-rush (Lomandra longifolia). Three approaches to mapping vegetation were evaluated, including: (i) a pixel-based image classification algorithm applied to the composite spectral wavebands of the images collected, (ii) manual digitisation of vegetation directly from images based on visual interpretation, and (iii) the application of a machine learning algorithm, LeNet, based on a deep learning convolutional neural network (CNN) for detecting planted Lomandra tussocks. The uncertainty of each approach was assessed via comparison against an independently collected field dataset. Each of the vegetation mapping approaches had a comparable accuracy; for a selected weed management and planting area, the overall accuracies were 82 %, 91 % and 85 % respectively for the pixel based image classification, the visual interpretation / digitisation and the CNN machine learning algorithm. At the scale of the whole island, statistically significant differences in the performance of the three approaches to mapping Lomandra plants were detected via ANOVA. The manual digitisation took a longer time to perform than others. The three approaches resulted in markedly different vegetation maps characterised by different digital data formats, which offered fundamentally different types of information on vegetation character. We draw attention to the need to consider how different digital map products will be used for vegetation management (e.g. monitoring the health individual species or a broader profile of the community). Where individual plants are to be monitored over time, a feature-based approach that represents plants as vector points is appropriate. The CNN approach emerged as a promising technique in this regard as it leveraged spatial information from the UAV images within the architecture of the learning framework by enforcing a local connectivity pattern between neurons of adjacent layers to incorporate the spatial relationships between features that comprised the shape of the Lomandra tussocks detected.

Keywords

interpretation, machine, visual, classification, pixel, images:, (uav), vehicle, aerial, unmanned, vegetation, island, mapping, techniques, approaches, evaluating, learning

Publication Details

Hamylton, S., Morris, R. H., Cabral Carvalho, R., Roder, N., Barlow, P., Mills, K. & Wang, L. (2020). Evaluating techniques for mapping island vegetation from unmanned aerial vehicle (UAV) images: Pixel classification, visual interpretation and machine learning approaches. International Journal of Applied Earth Observation and Geoinformation, 89 102085-1-102085-14.

Authors

Sarah Hamylton, Rowena H. Morris, Rafael Cabral Carvalho, N Roder, P Barlow, K Mills, and Lei Wang

Int J Appl Earth Obs Geoinformation 89 (2020) 102085

Contents lists available at ScienceDirect

Int J Appl Earth Obs Geoinformation

journal homepage: www.elsevier.com/locate/jag

Evaluating techniques for mapping island vegetation from unmanned aerial vehicle (UAV) images: Pixel classification, visual interpretation and machine learning approaches

S.M. Hamylton[a,*], R.H. Morris[a,b], R.C. Carvalho[a,c], N. Roder[a], P. Barlow[a], K. Mills[d], L. Wang[e]

[a] School of Earth, Atmospheric and Life Sciences, The University of Wollongong, NSW, 2522, Australia
[b] NSW National Parks and Wildlife Service, Unit G, 84 Crown Street, Wollongong, NSW, 2500, Australia
[c] School of Life and Environmental Sciences, Deakin University, Warrnambool, VIC, 3280, Australia
[d] 12 Hyam Place, Jamberoo, NSW, 2533, Australia
[e] School of Computing and Information Technology, University of Wollongong, New South Wales, NSW, 2522, Australia

ARTICLE INFO

Keywords:
Lomandra
Convolutional neural network
Five Islands nature reserve

ABSTRACT

We evaluate three approaches to mapping vegetation using images collected by an unmanned aerial vehicle (UAV) to monitor rehabilitation activities in the Five Islands Nature Reserve, Wollongong (Australia). Between April 2017 and July 2018, four aerial surveys of Big Island were undertaken to map changes to island vegetation following helicopter herbicide sprays to eradicate weeds, including the creeper Coastal Morning Glory (*Ipomoea cairica*) and Kikuyu Grass (*Cenchrus clandestinus*). The spraying was followed by a large scale planting campaign to introduce native plants, such as tussocks of Spiny-headed Mat-rush (*Lomandra longifolia)*. Three approaches to mapping vegetation were evaluated, including: (i) a pixel-based image classification algorithm applied to the composite spectral wavebands of the images collected, (ii) manual digitisation of vegetation directly from images based on visual interpretation, and (iii) the application of a machine learning algorithm, LeNet, based on a deep learning convolutional neural network (CNN) for detecting planted *Lomandra* tussocks. The uncertainty of each approach was assessed via comparison against an independently collected field dataset. Each of the vegetation mapping approaches had a comparable accuracy; for a selected weed management and planting area, the overall accuracies were 82 %, 91 % and 85 % respectively for the pixel based image classification, the visual interpretation / digitisation and the CNN machine learning algorithm. At the scale of the whole island, statistically significant differences in the performance of the three approaches to mapping *Lomandra* plants were detected via ANOVA. The manual digitisation took a longer time to perform than others. The three approaches resulted in markedly different vegetation maps characterised by different digital data formats, which offered fundamentally different types of information on vegetation character. We draw attention to the need to consider how different digital map products will be used for vegetation management (e.g. monitoring the health individual species or a broader profile of the community). Where individual plants are to be monitored over time, a feature-based approach that represents plants as vector points is appropriate. The CNN approach emerged as a promising technique in this regard as it leveraged spatial information from the UAV images within the architecture of the learning framework by enforcing a local connectivity pattern between neurons of adjacent layers to incorporate the spatial relationships between features that comprised the shape of the *Lomandra* tussocks detected.

1. Introduction

As unmanned aerial vehicles (UAVs), or drones, have become more affordable and the capability of the sensors that can be operated from them has improved, they have become more widely adopted platforms for acquiring aerial images with which to accurately map, better understand and manage environmental landscapes. The popularity and utility of UAV platforms stems largely from autonomous functionalities they allow, which minimise user intervention including the ability to plan and conduct surveys to collect aerial photography or remote sensing data across a broad spectral range, over an area interest. Examples of different sensor applications include the acquisition of thermal

* Corresponding author.
E-mail address: shamylto@uow.edu.au (S.M. Hamylton).

https://doi.org/10.1016/j.jag.2020.102085
Received 21 September 2019; Received in revised form 4 February 2020; Accepted 10 February 2020
Available online 03 March 2020

images that detect body heat to monitor and conserve wildlife (Gonzalez et al., 2016), and the use of multispectral cameras operating at blue and green wavelengths that can penetrate water to map submerged marine fauna (Colefax et al., 2017). Applications of vegetation remote sensing from UAVs include mapping aquatic vegetation (Husson et al., 2016), monitoring the condition of native vegetation (Lawley et al., 2016) and managing agricultural crops (Krishna, 2016). A wide variety of vegetation mapping sensors can be operated from a UAV platform, including hyperspectral sensors that detect reflectance at many wavelengths and can discern different plant species (Xie et al., 2008), the use of red and near-infrared wavebands to calculate indices that indicate the degree of vegetative ground cover (Ghazal et al., 2015) and characterisation of canopy structure, including texture and vegetation height with a light detection and ranging (LiDAR) sensor (Lefsky et al., 2002).

Several key developments made over the last decade have the potential to result in a radically new way of generating feature data from pixel-based images. Computational advances have increased the accessibility of low-cost machines with fast arithmetic units, opening up the scope for numerical approaches to machine learning. Furthermore, the "big-data" revolution has made large volumes of complex information readily available in environmental research, including satellite and UAV based remote sensing images that may be analysed computationally to reveal patterns and trends. Up until now, the variability and richness of natural features depicted as raster images, particularly the comparably coarse resolution of earth observation satellite images has presented a challenge to pattern recognition algorithms. However, the substantial increase in spatial resolution that has been introduced through the operation of UAV platforms at much lower altitudes, which have reduced pixels sizes from 30 m^2 to 3 cm^2, has rendered many smaller features amenable to detection via machine learning. Collectively, these developments are changing how remote sensing technology is applied at regional scales (ca 50 km^2) to better understand landscapes. This is particularly the case in dynamic environments that are subject to either natural or anthropogenically-induced changes, where deep learning techniques have the potential to not only identify features of interest, but to track how they evolve over time.

Classification in remote sensing involves the categorisation of response functions recorded in imagery (i.e. detected light that has reflected from the Earth's surface) as representations of real-world objects. In the context of the present study, classification transforms images collected from a UAV into a customised vegetation map. This process can be achieved through the application of either supervised or unsupervised image classification algorithms, by simply viewing, interpreting and manually annotating aerial images by digitisation (i.e. digitally tracing over features to be mapped), or through the application of a variety of machine learning approaches (e.g. decision trees, random forest classifiers or convolutional neural networks). Each of these approaches is subject to advantages and disadvantages. For example, object-based image classifiers have been successfully applied to UAV orthoimage mosaics collected by the DJI Phantom 4 to differentiate between tree crowns of wild pistachio and almond trees (Chenari et al., 2017) and to estimate grass biomass (Viljanen et al., 2018) drawing on the unique texture and colouring of these vegetation communities. While visual interpretation and digitisation of images has yielded reliable vegetation mapping results, such approaches are time both consuming and susceptible to the bias of the interpreter, as well as errors in the manual digisation of features (Barlow, 2018; Hamylton, 2017).

Several studies have employed machine learning algorithms to recognise vegetation, with a particular focus on detecting clusters of woodland forest or wetland vegetation rather than individual plants (Dujon and Schofield, 2019). Machine learning offers a fundamentally different approach to the processing routines available through most commercial image processing softwares, which rely on pre-programmed algorithms to classify input image data into an output map based on the relative statistical reflectance properties of their composite pixels. In the case of machine learning, the data and desired result are provided to a learning algorithm (a 'learner'), which then generates the algorithm that turns one into the other. For example, deep neural networks (DNNs) are composed of multiple layers between the input and output layers which collectively define the correct mathematical manipulation that generates the output from the input through a series of convolutions (LeCun et al., 2015). These algorithms are increasingly finding uses in remote sensing applications, although little is known about their performance in comparison to existing vegetation mapping approaches.

1.1. The use of convolutional neural networks for recognising objects in images

Machine Learning technology has developed in response to the rigidity of many computer programs in comparison with the world's infinite versatility (Domingos, 2015). In the case of feature detection from remote sensing images, one of the key challenges has been reliably recognising real-world objects from a large number of pixels. To date, this has largely been achieved using statistical classifiers that discern features or ground cover based on multiple reflectance values across different wavebands composing an image, or applying predefined rulesets to logically classify objects segmented from an image (Xie et al., 2008).

Convolutional neural networks (CNN) are a class of deep neural network machine learning algorithm that has met with success in various image analysis applications, including facial and recognition of handwritten characters (LeCun et al., 1990; Matsugu et al., 2003). Given an input image and a predefined training set of object categories, a detection algorithm can locate all the object instances falling within these categories across an image (Blaschke et al., 2008). It does so at a fine-grained, regional level of the image to recognise recurring patterns that present themselves across multiple pixels based on user guidance. In doing so, it is able to draw explicitly on useful signals that are apparent in the collective properties of pixels within an image. By interleaving convolutional and pooling layers, CNN algorithms have proven to be good at extracting mid- and high-level abstract features from raw images in large-scale image recognition, object detection, and semantic segmentation exercises (Zhu et al., 2017).

Given a database of images, feature detection algorithms can learn to detect commonly occurring features from the images, and one of the key challenges related to the application of machine learning for this purpose is finding out what is needed from initial assumptions, particularly how much data the learner algorithms require so that features can consistently be reliably detected from image data. This relates specifically to the amount of, and variability between, training instances used.

In the present study, we adopt a vegetation rehabilitation case study to evaluate how a CNN machine learning algorithm can learn to detect *Lomandra*, and how this compares to other commonly used approaches for vegetation mapping.

The present study aims to compare the advatages and disadvantages of three distinct approaches to vegetation mapping from UAV images by:

1 Mapping the vegetation of Big Island, with a particular focus on tussocks of the native mat-rush plant *Lomandra longifolia*, using the following three approaches:
   i
      i a pixel-based image classification method,
      ii visual interpretation and manual digitisation of individual *Lomandra* tussocks, and
      iii through the application of CNN machine learning object detection algorithms.
2 Evaluating the above three approaches to vegetation mapping, in

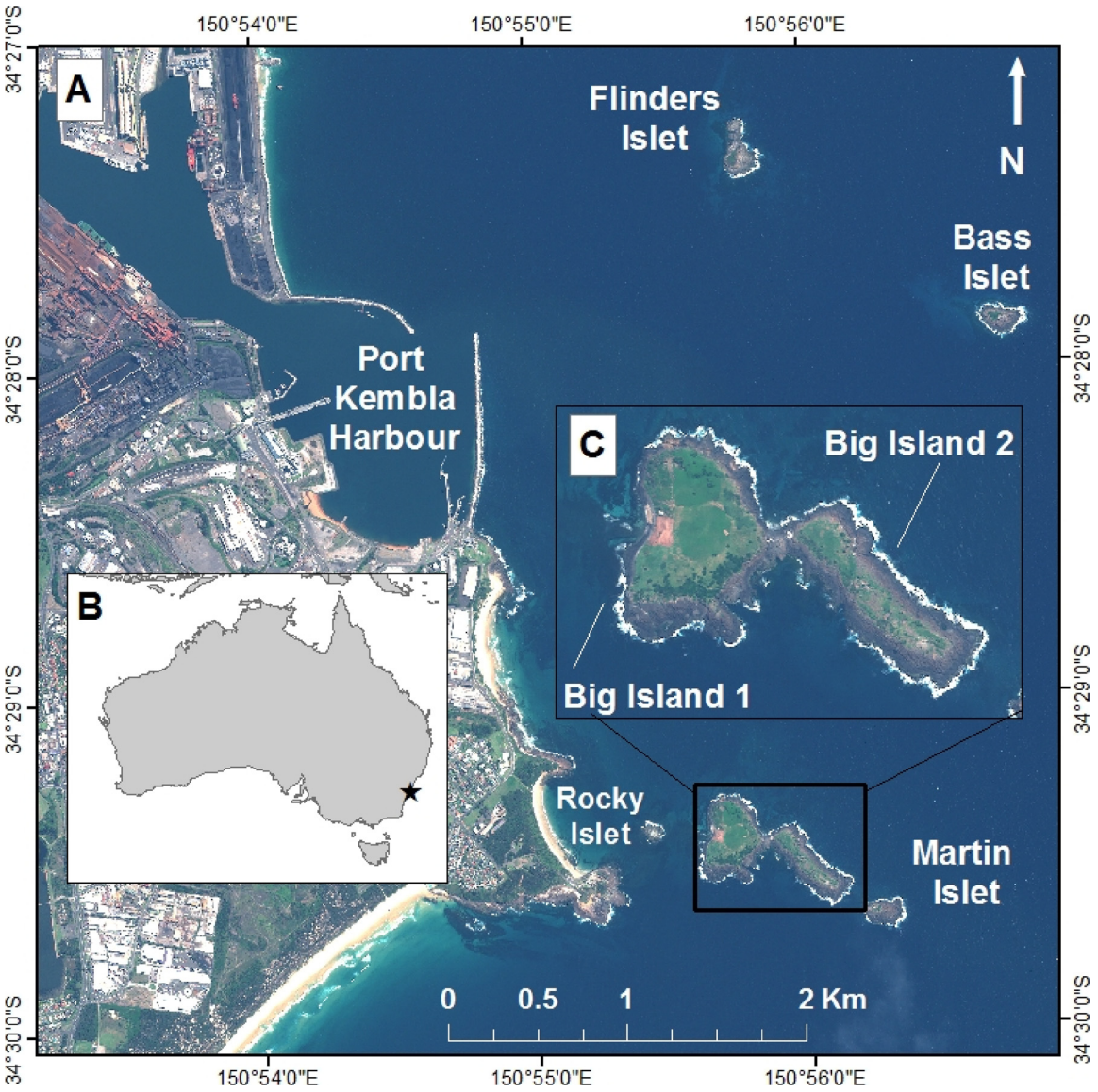

Fig. 1. (A) Port Kembla and the Five Islands Nature Reserve, (B) Study site location along the Eastern Australian Coastline, (C) Big Island 1 and 2, connected by a central rocky isthmus.

terms of the time taken for their implementation, their uncertainty as measured against a common ground referencing dataset and ascertaining whether statistically significant differences occur between their accuracies.

1.2. Study location: the Five Islands Nature Reserve

The Five Islands Group comprises Flinders Islet, Bass Islet, Rocky Islet, Big Island and Martin Islet, which collectively represent an area of approximately 0.26 km^2 that stretches 3.6 km offshore from Port Kembla, Wollongong in southern New South Wales (Fig. 1). The largest of the islands, Big Island (0.18 km^2) consists of two elevated islands joined by a low rocky isthmus that have been subdivided for management purposes into Big Island 1 and 2. The present study focuses on vegetation rehabilitation activities on Big Island 1 (herein, referred to as Big Island).

Wollongong experiences a warm temperate climate (Kottek et al., 2006), with an average annual rainfall and air temperature of approximately 1400 mm and 17 °C respectively. Precipitation is higher during the austral summer-autumn months (December to May) than winter-spring (June – November). Precipitation is the lowest in July with an average of 60 mm and reaches its peak of approximately 190 mm in March. February is the hottest (22 °C) and July is the coldest (11.9 °C) month of the year (Climate-Data, 2019). In 1938, Big Island was composed largely of exposed rock, soil and sand dunes, with 58 species of vegetation recorded, 40 of which were native and only 18 were deemed to be exotic (Davis, 1983). Since then, the ground cover has shifted from one dominated by sand and rock to a vegetated community that was initially comprised predominantly of native plant species but is now dominated by exotic species, particularly the dense grass Kikuyu (*Cenchrus clandestinus*) and creeper Coastal Morning Glory (*Ipomoea cairica*) (Figs. 2 and 3). Non-native vegetation in the form of Buffalo Grass (*Stenotaphrum secundatum*) was introduced to Big Island to reduce soil erosion by grazing goats and cattle. This began a history of significant human-induced changes to ground surface cover on the islands through the introduction of non-native plant species, land fires and mining for shell grit (Mills, 2015). The resulting shift in vegetative cover has resulted in severe habitat degradation for native seabirds that breed on the island.

In 1967, the Five Islands became a nature reserve under the *National Parks and Wildlife Act* (NSW). The islands are a site of significance to the Illawarra Aboriginal Community (NSW Department of Environment

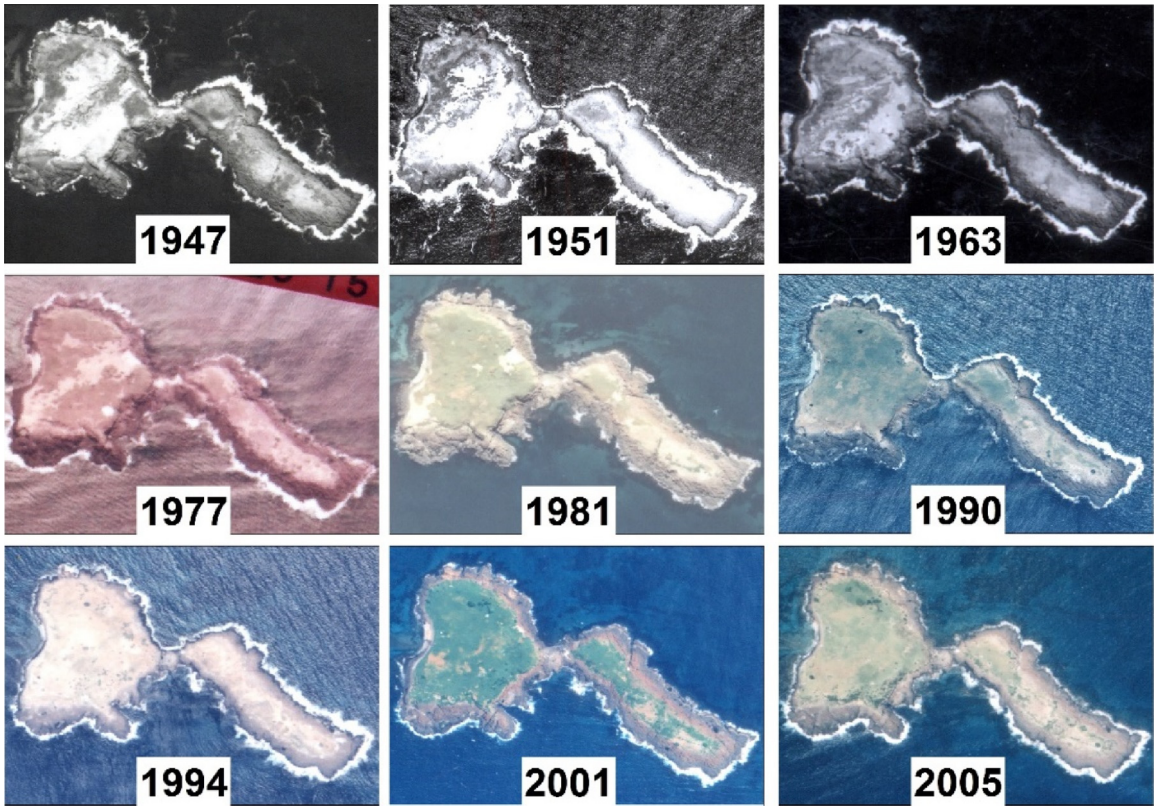

Fig. 2. Aerial photographs showing the gradual increase in vegetative cover of Big Island between 1947 and 2005 (photographs sourced from the School of Earth, Atmospheric and Life Sciences aerial photograph collection, The University of Wollongong). Rock outcrops border the entire island; Ground cover dominated by mostly sand (white) between 1947 and 1951, and subsequently by exotic vegetated species (grey in B&W / green in colour photographs). Brown indicates dry vegetation. (For interpretation of the references to colour in this figure legend, the reader is referred to the web version of this article.)

and Conservation, 2005), featuring in several dreamtime storie for the coastal Dharawal people (Organ and Speechley, 1997).

The islands provide important breeding habitat for many species of native shore and seabirds, including Wedge-tailed Shearwaters (*Ardenna pacifica*), Short-tailed Shearwaters (*Ardenna tenuirostris*), Sooty Oystercatchers (*Haematopus fuliginosus*; listed as a vulnerable species), Crested Terns (*Sterna bergii*), Silver Gulls (*Larus novaehollandiae*), Australian Pelicans (*Pelecanus conspicillatus*), White-faced Storm-Petrels (*Pelagodroma marina*) and Little Penguins (*Eudyptula minor*) (Carlile et al., 2017). The shearwaters, petrels and penguins dig burrows in the ground to lay their eggs and rear their chicks. Burrows are easily damaged by soil erosion, trampling or the current major problem of weed infestations, which trap the birds in their burrows or entangle their wings and legs. The rehabilitation of island vegetation was largely initiated due to the damage caused to burrowing seabirds.

1.2.1. Vegetation rehabilitation at Big Island

The original, pre-European vegetation on Big Island has been replaced with a dense weed cover following fires, clearing and weed invasion (Mills, 1990). From the late 1960s, a dense sward of Kikuyu Grass has spread and dominated the whole island. Most recently, the creeper Coastal Morning Glory has invaded part of Big Island. In 2014, a vegetation rehabilitation program was initiated by NSW National Parks and Wildlife Service in collaboration with Berrim Nuru Environmental Service of the Illawarra Local Aboriginal Land Council. This involved a staged weed removal followed by revegetation of Big Island for five focussed vegetation rehabilitation areas. Weed removal was undertaken by four operations involving helicopter aerial applications of glyphosate 360 g L^{-1} Manual replanting with a range of native species has occurred through a large-scale effort that has seen approximately 23,400 individual seedlings between 2015 and 2018 in focussed management areas. These were primarily tussocks of *Lomandra longifolia* due to their suitability as a ground cover that provides protection for seabirds without damaging the birds or their burrows. This species grows as a tussock of long leaves, to over 1-m long (see Fig. 3D). Due to this planting effort, along with natural expansion following the killing of the Kikuyu sward, the cover of native plants has increased substantially on Big Island (Mills, 2015).

2. Methods

2.1. Fieldwork: Ground referencing and UAV survey methods to support vegetation mapping

2.1.1. Ground referencing

Several field trips (summarised in Fig. 4) were undertaken on Big Island to collect *in-situ* ground referencing records of vegetation cover to assist with the development of digital vegetation maps, alongside aerial UAV surveys. These were timed to occur before and after aerial weed sprays in 2007 and 2018. In both years, the first trip occurred just days prior to the Glyphosate 360 g L^{-1} helicopter spray (April 2017 and May 2018) for the purpose of eradicating invasive weeds on Big Island, with a second trip three months after the aerial spray (July 2017 and July 2018).

Ground referencing photographs were collected on four separate fieldtrips as training and validation data respectively. On each trip, photographs recorded information on the vegetative land cover across the whole island. Photograph locations were recorded to 5 m XY positional accuracy. These reference photographs were then used for training the automated mapping algorithms (in the case of mapping approaches 1 and 3). In addition to this, half of one common set of ground reference photographs, shown in red on the May 2018 image

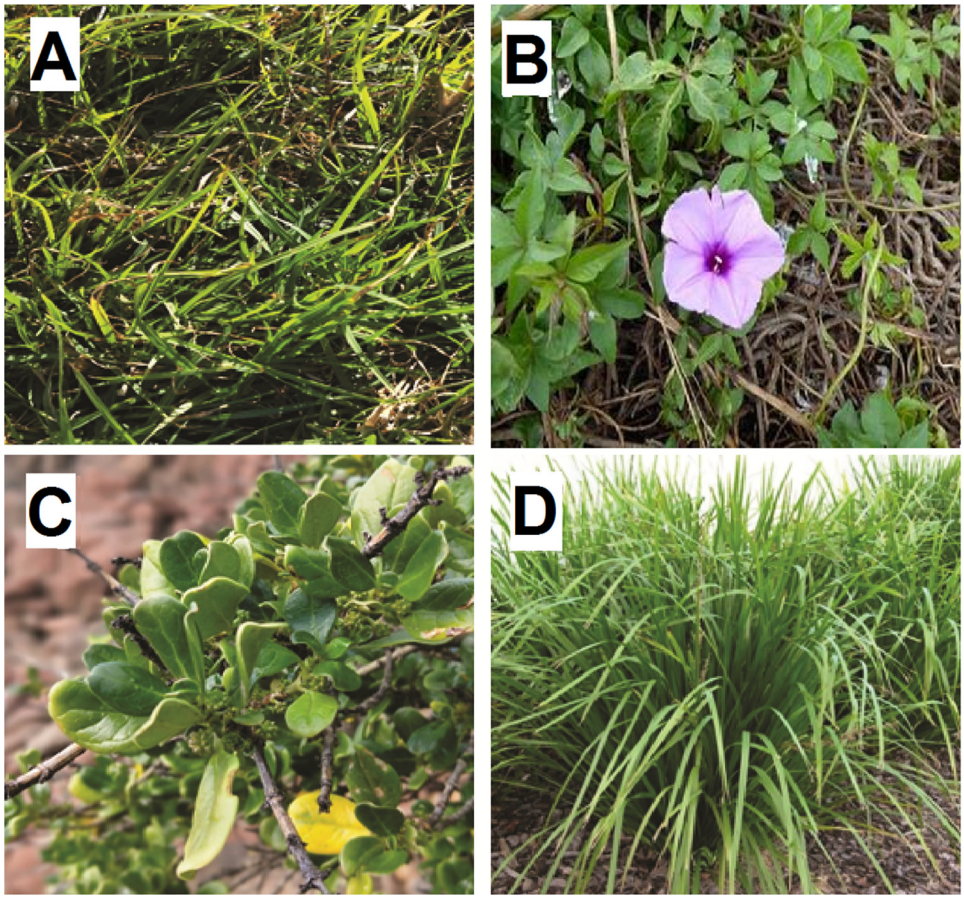

Fig. 3. Plant species targeted in the rehabilitation program. (A) Invasive weed Kikuyu Grass (*Cenchrus clandestinus*). (B) Invasive weed creeper Coastal Morning Glory (*Ipomoea cairica*). (C) Leaves of the woody weed Mirror Bush *(Coprosma repens)* and (D) Planted tussocks of the native *Lomandra longifolia.*

(Fig. 4), was employed to compare all three mapping approaches via accuracy assessment.

2.1.2. Unmanned aerial vehicle surveys

A DJI Phantom 4 UAV was used to acquire aerial images with a FC330 camera, using a built-in 1/2.3″ CMOS sensor, with a lens field of view of 94°, 20 mm (35 mm format equivalent), which captures images at 12.4 megapixels (MP). Images were captured at nadir, i.e. perpendicular (90° ± 0.02°) to the ground surface. The UAV was flown at 70 m above sea level along an autonomous, pre-programmed flight path to ensure the entire study area was included, with sufficient overlap between adjacent images to avoid gaps and allow subsequent photogrammetric processing (Table 1).

The raw images of each flight were collated into an orthomosaic using the photogrammetric software Agisoft Photoscan Professional (AgiSoft, 2014). The overall orthomosaic was constructed by applying feature matching and triangulation to a series of photographs for which the approximate x, y coordinate information had been captured in the associated Exchangeable Image File (EXIF, vision positioning system accuracy of ± 0.3 m). Feature matching involved detecting and matching clearly visible points representing the same feature from at least three different perspectives. Triangulation was used to adjust for camera orientation and focal length to produce a point cloud, which was then processed into a continuous mesh. To further improve locational accuracy, 17 visible targets were established at permanent features around the island periphery and interior (Fig. 4) including rocks and man-made structures as ground control points (GCPs), for which x, y and z coordinates were measured with a differential GPS (accuracy ± 0.32 m). A further georectification was then performed to bring the image mosaic into line with the GCPs.

2.2. Vegetation mapping approach 1: Pixel-based image classification

For each of the four mapping campaigns, all *in-situ* photo records were viewed independently and assigned a class with respect to the land cover classification scheme employed. This grouped all possible ground covers into one of seven classes: rock, water, Kikuyu Grass, Coastal Morning Glory, Mirror Plant (*Coprosma repens*) / Bitou Bush (*Chrysanthemoides monilifera rotundata*), *Lomandra* or other native vegetation and dead vegetation. Half of the ground referencing photographs collected were used to define training areas to supervise the image classification, the remaining half were used to assess and interpret the accuracy of the vegetation map.

A supervised classification was performed in ArcMap10.4.1 using a maximum likelihood parametric rule on the red, green and blue bands of the aerial images acquired by each UAV survey. The classified output was a single thematic layer that was subsequently interpreted with respect to the ground referencing dataset from the photo records. A final map of seven classes was produced by merging some of the output classes on the basis of spectral similarity and contextual editing (Mather and Koch, 2011). For the purpose of the vegetation mapping, the non-vegetation classes of rock and water were clipped from the outside of the map.

2.2.1. Assessment of pixel-based image classification accuracy

A validation exercise assessed the accuracy of digital maps generated from the pixel-based image classification by comparing the land cover specified by the digital thematic map for May 2018 to the land cover that was visually interpreted from the independent ground referencing photographs taken for this time period. To enable meaningful comparison of corresponding output maps with the other approaches,

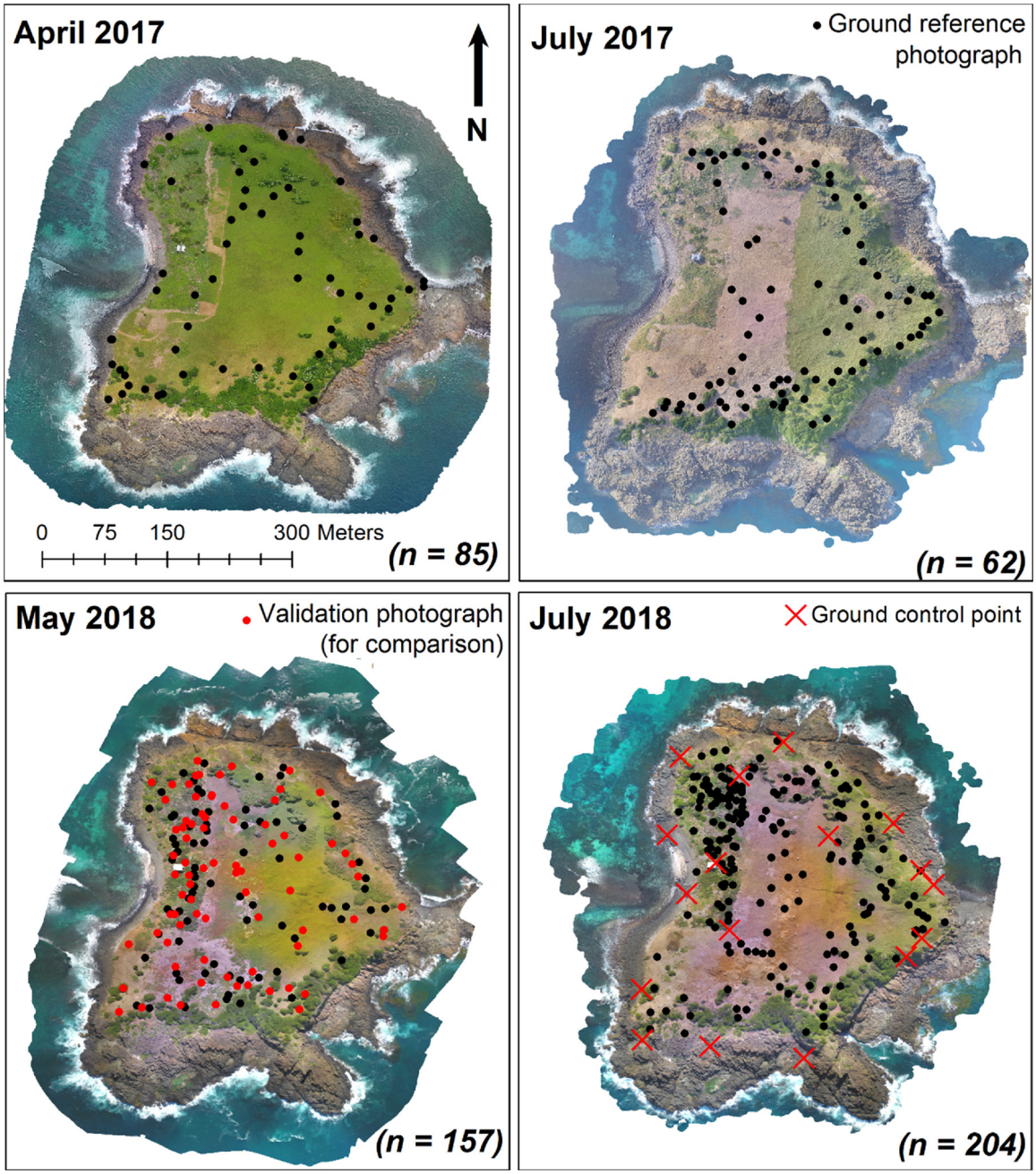

Fig. 4. Aerial mosaics of UAV survey images acquired before (left hand side) and after (right hand side) aerial weed spraying at Big Island. Dots indicate *in-situ* photographs taken as ground reference information (training and validation data) to support vegetation map production (black) and validation (red), while red crosses (July 2018) indicate ground control points (GCPs) collected for evaluating the positional accuracy of the UAV images. (For interpretation of the references to colour in this figure legend, the reader is referred to the web version of this article.)

the producer's accuracy of the *Lomandra* class mapped was calculated as the proportion of ground referencing photographs collected *in-situ* that were identified as *Lomandra* that were also assigned to the *Lomandra* class as the digital map (Congalton and Green, 2008).

2.3. Vegetation mapping approach 2: Visual interpretation and manual digitisation of plants

The visual interpretation and manual digitisation of vegetation focussed on the ground cover of *Lomandra longifolia* tussocks as visible in the May 2018 orthomosaic. Tussocks of *Lomandra* were visually identified, based on the size, shape and colour, digitised from the Big Island orthomosaic on a screen at a scale of 1:50 and recorded as digital vector data points. A point shapefile was created to represent *Lomandra* tussocks and assigned spatial referencing information to match that of the UAV images.

Fully grown *Lomandra* tussocks were identified (average diameter of around 1.2 m, earthy green colour, circular shape with a central vertex), as well as juvenile *Lomandra* tussocks that were large enough to be interpreted from the aerial image. Where tussocks has clustered together, individual plant sizes and shapes were estimated based on the position of each plant centre.

2.3.1. Assessment of visual interpretation and manual digitisation accuracy

Probabilistic methods are an established technique for assessing the uncertainty of manually digitised vector datasets generated from the

Table 1
Flight and image processing parameters for the UAV surveys of Big Island.

Parameters	Big Island
Dates	19 April 2017, 29 July 2017 23 May 2018, 7 July 2018
# Images	281
Area	0.12 km^2
Flying altitude	70 m
Image frontlap	75 %
Image sidelap	75 %
Number of GCPs	17
Post-processed GPS accuracy (July 2018)	0.32 m
Alignment accuracy	High
# Tie points	36,817
XY error of GCPs following Photoscan processing (July 2018)	5.23 cm
Resolution (orthomosaic)	3.0 cm

visual interpretation of images (Hamylton, 2017). Broadly, these methods use repeated attempts to interpret and digitise the same features to estimate the spread, or variability, of the resultant vector data as a measure of uncertainty.

A probabilistic estimate of uncertainty of the digitization of *Lomandra* was evaluated from the statistical distribution of multiple repeat digitisations of *Lomandra* plants. To do this, 30 volunteers with expertise in GIS analysis from the University of Wollongong were asked to digitise all the *Lomandra* plants inside a selected weed management area of Big Island (0.01 km^2) over a standardised period of fifteen minutes. These data were then used to create a frequency histogram of the results by binning the estimated numbers of *Lomandra* (ranging between 0 and 840) and statistical uncertainty metrics were calculated, including the statistical mean, range, standard deviation, standard error, 95 % confidence intervals and the root mean squared error (Barlow, 2018).

2.4. Vegetation mapping approach 3: Application of a CNN machine learning algorithm

A third approach to the detection of *Lomandra* tussocks applied a gradient-based learning algorithm called LeNet to the May 2018 orthophotomosaic. This was trained by the ground referencing data collected in the same year (Fig. 4, black dots). The decision was made to recognise individual tussocks of *Lomandra* rather than continuous cover of other vegetation types (e.g. Kikuyu) as the LeNet algorithm is designed for object recognition. Gradient-based approaches to learning operate by minimising a function between an output pattern (i.e. a detected feature) and set of adjustable parameters with respect to a given input (i.e. an image). They use analytical computations to generate a smooth, continuous function to estimate the discrepancy between the correct output and that produced by the algorithm (often termed the 'loss') from the gradient of this loss function with respect to adjustable parameters.

A typical CNN algorithm for feature recognition is made up of a staged series of convolutions and maxpooling that collectively define the relationship between the output (detected feature) and the input (raw image) (see Fig. 5). The detailed architecture of the LeNet CNN algorithm is described elsewhere by LeCun et al. (1998).

Examples of the features to be detected were centred on the input field using a series of photographs in which the locations of 1194 *Lomandra* plants had been labelled. The whole image was partitioned into 45 tiles (of size 2400 by 1900 pixels), half of which formed a training set and the remaining half formed an independent test set.

The training set of 'positive examples' (i.e. regions where *Lomandra* was present) was generated by cropping many small corresponding regions (sized 64 by 64 pixels) centred on the *Lomandra* plants. A training set of negative examples (i.e. regions where *Lomandra* was not present was generated by sliding a window of the same size over the training photographs and identifying windows that did not significantly overlap with positive examples (i.e. $<$ 1000 pixels overlap) as negative examples. Thus, overall training datasets of 1194 positive and 174,243 negative examples were created.

The LeNet convolutional network incorporated three design elements (local receptive fields, shared weights and spatial maxpooling) that enabled features to be detected at various scales and with potential image shifts and distortions. Local receptive fields were iteratively assessed via a 'sliding stride' function across sub-regions of an entire image. This identified regions of interest inside a 64 $\times$ 64 pixel window (i.e. covering 1 m on the ground) that was passed at 10-pixel stride increments across the entire test patch image. In this way, network neurons extracted elementary features, the locations of which were collectively recorded on a uniformly weighted feature map. These were combined in subsequent layers to detect higher-order features and for each location, the content of the window was categorised as '*Lomandra*' or 'not *Lomandra*' (see Fig. 5). A complete convolutional layer was composed of several feature maps (each with different weight vectors applied) and the network was built up through sequential implementation of feature maps, complete with their connection weights, followed by an additive bias and a squashing function (LeCun et al., 1998). Thus, each output feature map was connected to an input feature map and the term 'convolution' corresponded to the mathematical operation that summed all the individual convolutions of all inputs through their corresponding filters.

The detection exercise took 600 s to run on an Intel Core i7-3820 central processing unit (3.60 GHz x 8, Memory 31.4GiB). For each object (i.e. individual *Lomandra* tussock), the detection algorithm predicted the bounding box of each tussock in an image through implenetation of the detection algorithm. Maxpooling was applied to each feature map layer to downgrade the precision with which the positions of distinctive features were encoded into feature maps. This reduced the sensitivity of the output to shifts and distortions of the input by averaging out features locally. Finally, to improve detection accuracy and remove redundant windows, non-maximum suppression (NMS) was applied to merge multiple detected windows containing *Lomandra* that had significant overlapping.

2.4.1. Assessment of CNN machine learning algorithm accuracy

The accuracy of detection results was assessed by comparing plants detected by the algorithm with those in the test set, and calculating true positive rates (TPR), false negative rates (FNR), false positive rates (FPR) and true negative rates (TNR). The performance of the algorithm was expressed as a percentage accuracy, calculated as the proportion of positive detections that were correct (i.e. TPRs). This metric aligned with the accuracy assessments of the other approaches, while also avoiding disproportionate influence from the large number of true negative rates.

2.5. Comparison of the three vegetation mapping approaches

A subset of the May 2018 image which corresponded to a weed management and planting area of the Big Island Rehabilitation Program (0.01 km^2) was selected for inter-comparison of the three approaches. In this area, maps made by each of the three approaches were assessed for accuracy based on the same ground referencing dataset (see Fig. 4, red dots).

A bootstrapping method was adopted to enable a formal statistical comparison of producer's accuracy across the three Lomandra vegetation mapping approaches. For each mapping approach, the producer's accuracy for Lomandra was calculated twenty five times from the 74 validation ground referencing points across the whole island (red dots on Fig. 4), Each calculation was performed on a subset of the validation dataset from which 10 random points had been omitted. Producer's

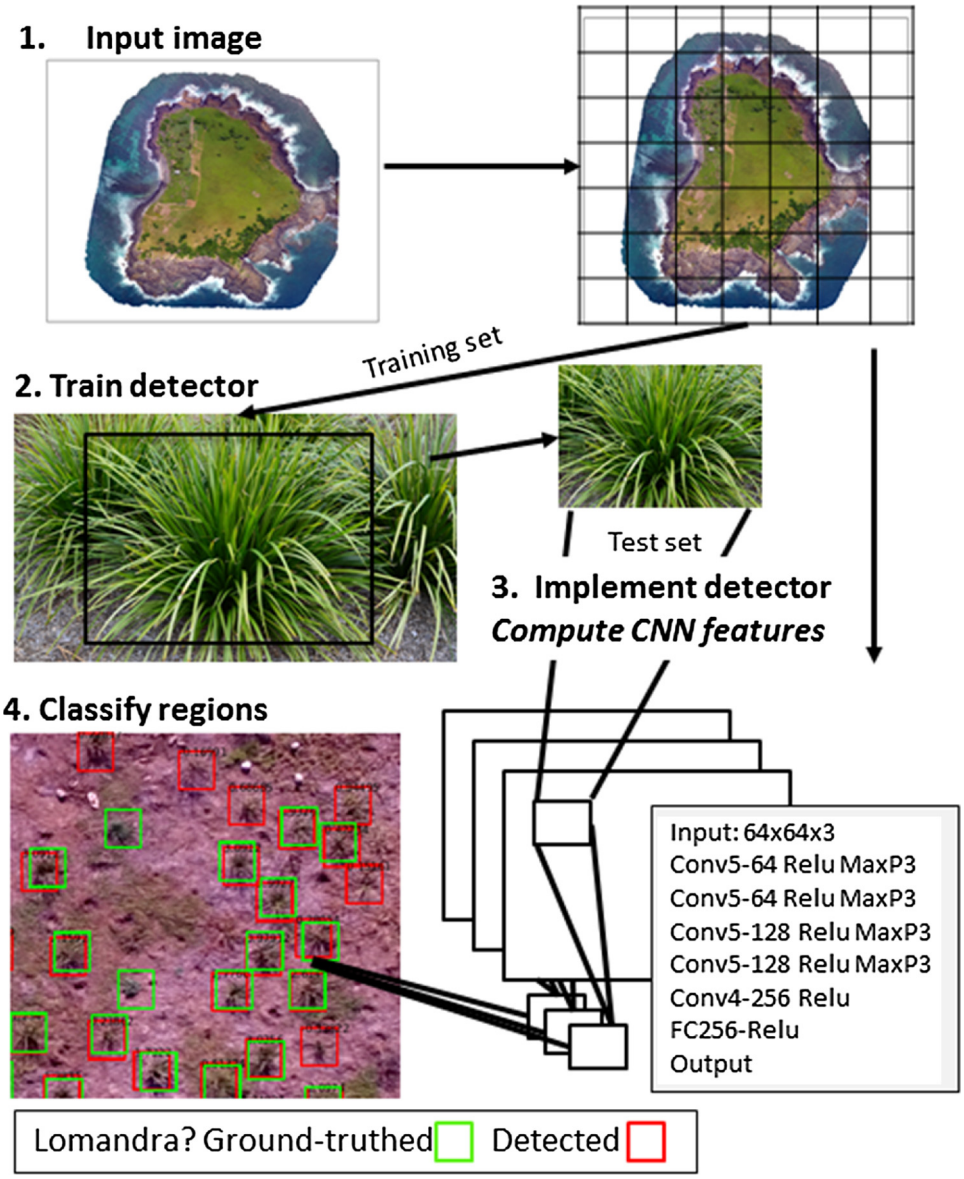

Fig. 5. Process flow diagram illustrating the four-step implementation of the convolutional neural network machine learning algorithm on UAV images to detect *Lomandra* plants. The procedure begins with image preparation through subdivision, training of the detection algorithm on a set of pre-dertermined *Lomandra* plant images, implementation of the detection algorithm on a test set of images and subsequent classification of detected features into *Lomandra* plants through a series of convolutions (Conv), their output layers (Rectified Linear Units, Relu) and subsampling via maxpooling (MaxP).

accuracy was defined as the proportion of ground referncing photographs collected *in-situ* that were identified as *Lomandra* that were also mapped as *Lomandra* using the different mapping approaches. This iterative approach enabled estimation of a sampling distribution for the producer's accuracy metrics for each vegetation mapping approach, from which standard error could be derived. In turn, the differences between the mean accuracy metrics as grouped by mapping approach, could be tested for statistical significance using a one way analysis of variance (ANOVA) using the statistical package SPSS. Overall, this revealed whether or not there were statistically significant differences between the accuracy of the three Lomandra mapping approaches.

3. Results

3.1. Vegetation mapping approach 1: Pixel-based image classification

The pixel-based image classifications produced digital vegetation maps that characterised the full extent of Big Island into five vegetation classes, with seven ground cover classes in total (including water and rock platform, which were subsequently clipped from the digital vegetation map, Fig. 6). Producer classification accuracies for *Lomandra* ranged from 74 % to 85 % for the complete island area.

3.2. Vegetation mapping approach 2: Visual interpretation and manual digitisation of plants results

The visual interpretation and digitisation took approximately eight hours in the GIS laboratory. A total of 1351 individual *Lomandra* tussocks were manually digitised across Big Island, falling largely inside the weed management area in the north western sector of the island (see Fig. 7a). Of these plants, 56 coincided with ground referencing images of *Lomandra*, for which 52 had been visually identified and recorded as *Lomandra*, yielding a producer accuracy of 93 %.

The repeat digitisation exercise undertaken by 30 trained digitisers yielded a wide statistical spread in the estimations of the number of *Lomandra* plants inside the weed management area (Fig. 8), ranging

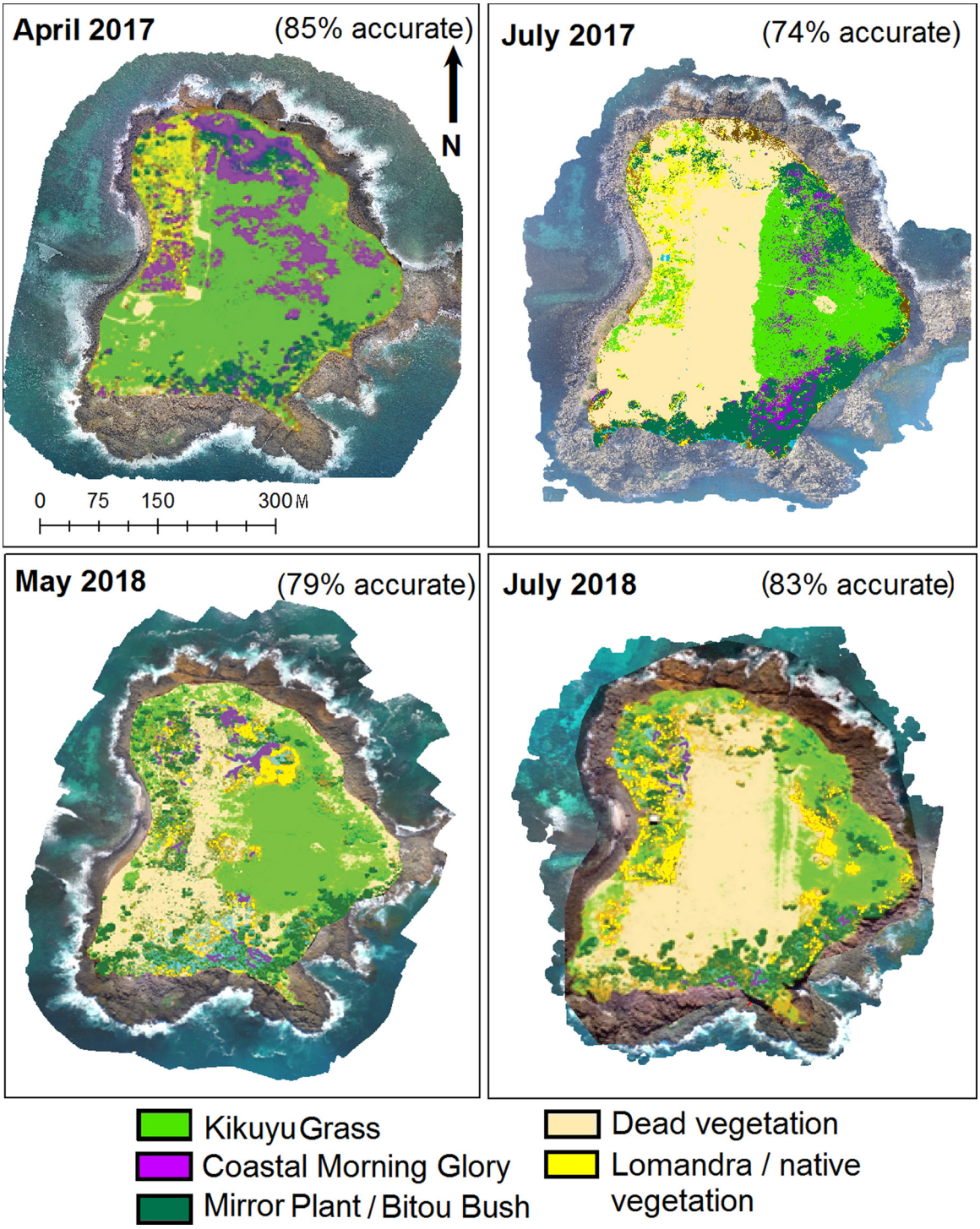

Fig. 6. Pixel-based classifications of the vegetation cover for Big Island, before (left) and after (right) aerial weed sprays undertaken in 2017 and 2018 (see Fig. 4 for raw image mosaics). Note that the water and rock platform classes have been removed to emphasise the classified vegetation.

from 456 to 754, with a standard deviation of 86 and a standard error of 17.

3.3. Vegetation mapping approach 3: Application of a machine learning algorithm

Results from the application of detection algorithm are summarised in Table 2. Of the 1351 *Lomandra* plants, the algorithm detected 1103 (81 % TPR) as true positive objects while wrongly detecting 427 non-*Lomandra* windows as *Lomandra* (0.05 % FPR) and failing to detect 248 plants (18 % FNR). Fig. 9 illustrates an image employed in the test site, with the detection results overlaid. The spatial coincidence of the green and red window locations, which represent the ground truth and successfully detected *Lomandra* locations respectively, illustrates the high performance of the detection algorithm. Large areas devoid of *Lomandra*, particularly those associated with low-growing Kikuyu Grass were correctly classified as negative objects, i.e. not *Lomandra* plants (Fig. 9). The detection algorithm also performed with a high success rate in areas represented by a more diverse array of vegetation types, such as mosaics of *Lomandra* plants interspersed with the native

Table 2
Summary of detection results via comparison of plants detected by the algorithm and those in the test set, including true positive rates (TPR), false negative rates (FNR), false positive rates (FPR) and true negative rates (TNR). Shaded boxes indicate correctly detected objects.

	Ground truth (test set)		
Detection algorithm		Positives	Negatives
	Positives	1103/1351 (TPR = 82 %)	427/ 945760 (FPR = 0.05 %)
	Negatives	248/1351 (FNR = 18 %)	945333/945760 (TNR = 99.95 %)

succulent creeper Pig Face (*Carpobrotus glaucescens*), dead vegetation and Mirror Bush *(Coprosma repens)*. The falsely positively classified objects (0.05 % FPR) primarily arose from the confusion of *Lomandra* with dead vegetation.

3.4. Comparison of vegetation mapping approaches

The three mapping approaches had comparable accuracies inside the weed management and planting area. The manual digitisation of *Lomandra* plants took eight hours, which was the longest time, while the automated approaches were faster, taking two hours and two hours 15 min for approaches one and three respectively (see Fig. 10).

Producer's accuracy for mapping *Lomandra* across the whole island was very similar to the accuracies estimated for the weed management and planning area. Analysis of variance in producer's accuracy across each of the three approaches for mapping Lomandra, yielded an F-statistic of 24.38 ($p < 0.001$). This meant that variation was significantly greater than expected between the group averages, suggesting that the accuracy with which Lomandra was mapped was statistically significantly dependant on the mapping approach employed (Fig. 11).

4. Discussion

4.1. Evaluation of the vegetation mapping approaches

The pixel-based image classifications accurately summarised vegetation cover for the full areal extent of Big Island (across the four surveys, accuracies ranged from 74 to 85 %). This is a surprising finding given that the spectral capability of the three-band RGB sensor for vegetation mapping is limited. The absence of an infra-red band potentially constrains the ability to discern vegetation from other, non-vegetative landcovers based on their spectral reflectance. Typically, the spectral radiances in the red and near infrared wavelength regions of the electromagnetic spectrum detect photosynthetically active radiation and have the greatest utility for reliably distinguishing vegetation from other land cover types. Nevertheless, in this exercise supervised pixel-based classification algorithms reliably mapped seven classes, five of which were vegetation (Fig. 6). This suggests that the three-band RGB aerial photographs were fit for the purpose of distinguishing between coarse vegetation types.

The map derived by manually digitising *Lomandra* plants had a comparable level of accuracy to the image classification, although it was focussed on only one of the vegetation types depicted in the map generated through the pixel based classification (i.e. in the first approach, *Lomandra* tussocks were represented as a more general component of the "native vegetation class"). In the management context of the broader vegetation rehabilitation program (section 1.2.1), it can be useful to track the progress of planted native *Lomandra* tussocks, and to monitor their ongoing health to answer practical questions, such as "how many healthy individual tussocks are there on the island, where are they, and where should be place our planting efforts?" Such focus comes at the exclusion of other plants. To capture the same level of complexity as the pixel-based map, which had five vegetation classes, an equal amount of effort would need to be invested in the visual interpretation and manual digitisation of other types of vegetation, which would likely take 40 h (i.e. eight hours multiplied by five classes), across the whole island.

From a starting point of images where *Lomandra* tussocks were labelled with the correct categories, LeNet defined functions that characterised each one, then accurately applied these to unlabelled images. While multi-layer convolutional networks trained using gradient-based approaches have a proven ability to learn complex, high-dimensional non-linear mappings from large collections of examples, this is the first time they have been successfully applied to detect individual *Lomandra* tussocks from mosaicked UAV images across a complete island landscape. This is a noteworthy finding because the structure from motion photogrammetric technique employed to mosaic together individual UAV images via feature matching introduces distortions into the image, which may have changed the shape of the *Lomandra* tussocks within the background matrix of ground cover (Barlow, 2018). Yet the long, thin blades of these plants emanating from a single centre point could be defined by the CNN learner as a distinctly recognisable feature across collective pixels.

The ability of the CNN learner algorithm to recognise features depends heavily on the user providing an appropriate set of training instances, which has historically been a difficult task in applications such as street surveillance or medical x-ray images (LeCun et al., 1998). Because drone images are acquired at a distance that is typically further from the subject than most photographs (i.e. a flight altitude of 60 m), they typically cover a large ground footprint (in this case, 120 m^2) and therefore include multiple instances of the same feature that can be utilised in the training process to overcome this challenge.

Two additional key features of UAV image datasets combine to make them particularly amenable to the application of CNN machine learning. Firstly, the raster grids are configured at a high enough spatial resolution to clearly resolve individual plants. *Lomandra* tussocks are typically sized around 1 m^2, which can clearly be distinguished from an image with a spatial resolution of three cm. Secondly, the raster grid configuration of UAV images retains important spatial contextual information. Because the convolutions pass local filters over the input image space, they exploit the spatial structure present in natural landscape images. While other machine learning techniques such as decision trees have been used for mapping invasive grasses in arid environments (Sandino et al., 2018) and random forest classifiers detected weeds in maize fields (Gao et al., 2018), these machine learning frameworks are based on inverse deduction. They draw on the spatial domain of an image to segment pixels based on their neighbourhoods before employing logical reasoning to classify segments. The learning frameworks of these machine learning algorithms therefore do not utilise contextual information or emergent patterns from collective pixels in the same manner.

A distinctive feature of CNN algorithms is that they have a specialised learning architecture based on the particular task for which they are designed that draws on local connection patterns between features, enforcing a local connectivity pattern between neurons of adjacent feature map layers within the convolutions (LeCun et al., 1998). Thus, the spatial relationships within and between receptive fields are explicitly built into the feature extractor in a way that is distinct from conventional image processing algorithms (e.g. supervised classification algorithms).

Several issues adversely affected the accuracy of the detection

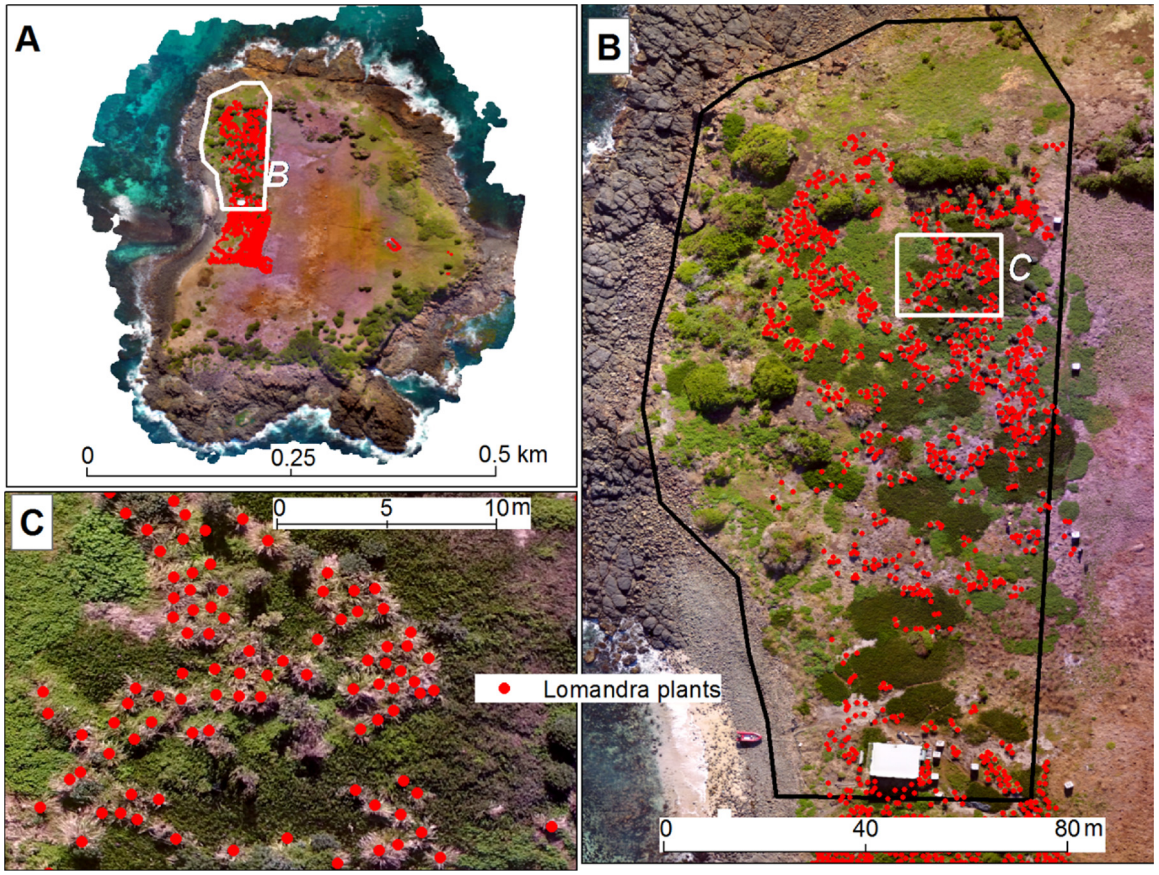

Fig. 7. (A) *Lomandra* plants (depicted as red dots in each picture) digitised across Big Island in May 2018 (white inset show area depicted in B), (B) Distribution of *Lomandra* the weed management and planting area of the Big Island Rehabilitation Program (white inset shows area depicted in C), (C) *Lomandra* plants at a scale of 1:50. (For interpretation of the references to colour in this figure legend, the reader is referred to the web version of this article.)

algorithm, which could be further refined for the detection of *Lomandra* tussocks. The performance of an object detection model is inherently linked to the number of representative images, and the extent to which they are representative of the complete range of scenarios in which the object appears (e.g. in different weather and lighting conditions) (Bottou and Vapnik, 1992). There need to be enough data to learn general patterns and this relatively limited set of positive examples could limit the efficacy of the classifier in recognising the variable form of *Lomandra* tussocks. In this case there was a very high number of negative training examples compared to the number of positive training examples i.e., 945,760 vs. 1351. Also, only the centres of the plants were manually labelled for the training exercise, thus, no information was incorporated on the individual plant sizes, which were approximated to be 64 × 64 pixels (i.e. 1 m^2). Detection performance could likely be improved by building in more information to capture the complexity of these *Lomandra* tussocks, employing more advanced CNN

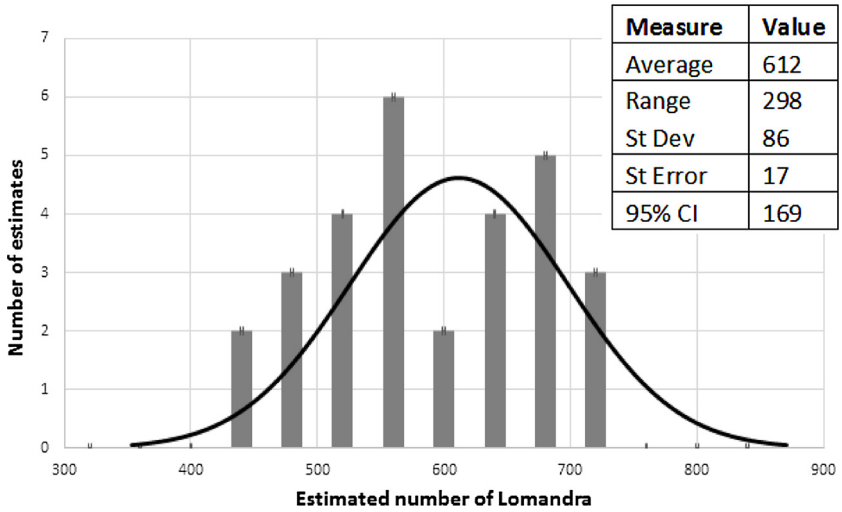

Fig. 8. Frequency histogram of thirty estimates of the abundance of *Lomandra* plants in the weed management and planting area of Big Island (see Fig. 7 for location). Inset table: Statistical uncertainty estimates based on thirty repeat digitisations of *Lomandra* plants inside the weed management and planting area.

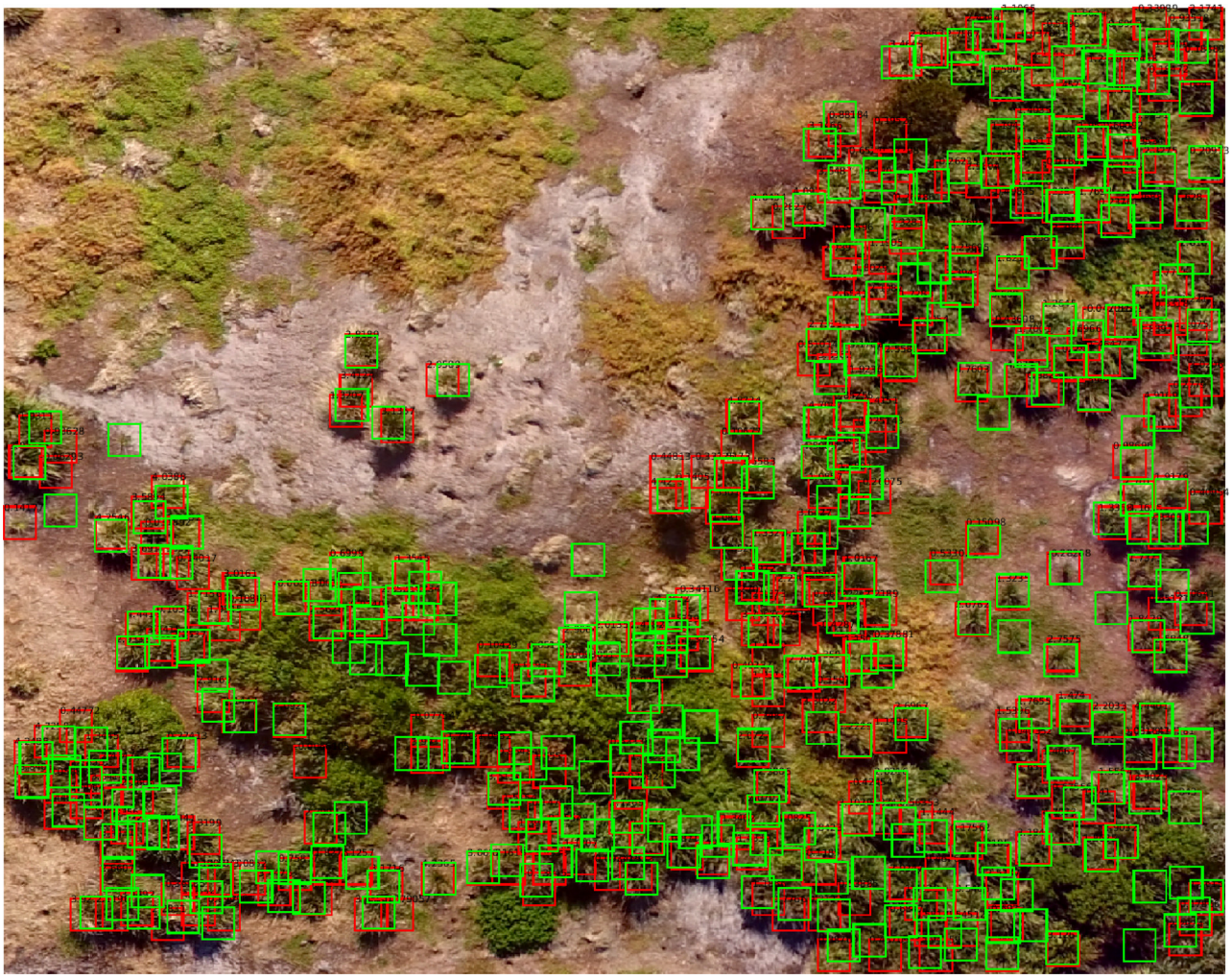

Fig. 9. Example test set image with ground-truthed *Lomandra* plants (green boxes) and plants correctly identified by the detection algorithm (red boxes). (For interpretation of the references to colour in this figure legend, the reader is referred to the web version of this article.)

models. Finally, the illumination in the different photographs varied across the whole island, making some of the plants difficult to detect. This confounding effect could be mitigated by planning UAV survey times to coincide with solar zenith, so that shadows and ambient light variability are minimised (Mather and Koch, 2011).

4.2. Comparison of the vegetation mapping approaches

In terms of accuracy, each of the mapping methods performed reasonably well, with all accuracies falling between 74 % and 91 % for the selected weed management and planting area. The comparative ANOVA exercise indicated a statistically significant difference in the performance of the three mapping approaches, as estimated via the producer's accuracy of the Lomandra maps across the whole island. Average producer accuracies calculated in the bootstrapping exercise were comparable to those estimated within the weed management and planting area, with the three mapping approaches ranking in the same order, i.e. visual interpretation and manual digisation was found to be the most accurate approach (approach 2, 89 % average producer's accuracy), followed by the machine learning CNN algorithm (approach 3, 84 % average producer's accuracy) with pixel-based image classification emerging as the least accurate (approach 1, 79 % average producer's accuracy).

Although they had similar levels of user-reliability, as digital vegetation maps they represented fundamentally different types of information, both in terms of data format and the vegetation they represented. The raster map derived from the image classification (approach 1) subdivided the entire vegetation community into five classes, providing a continuous indication of vegetative cover for the entire land area of the island. The feature maps provided information on a single type of vegetation (*Lomandra*), derived from the manual digitisations and machine learning algorithms (approaches 2 and 3, respectively). Working with data stored in these two fundamentally different formats is subject to a range of practical advantages and disadvantages (summarised in Table 2.1, pg 35 of Barlow, 2018). Notably, raster grids provide continuous data over a large geographic area, which can depict gradients of change well, but they store information less precisely than feature data and potentially incorporate redundant information in geographic areas of less management interest. Conversely, feature data are more thematically-focussed, highly localised and typically incorporate less data redundancy, generating smaller file sizes that are computationally less intensive to process.

Both of the automated mapping approaches (i.e. the pixel based supervised classification and the LeNet machine learning algorithm utilised in approaches 1 and 3) were faster to run than the manual digitisation. The time invested in running them was spent "training" the algorithm, i.e. calibrating it to run in an automated fashion by training either a spectral classification or a feature detection algorithm. Once trained, such algorithms have utility beyond the present mapping exercise as they can be applied to other images, thereby heightening their practical value for vegetation management. For example, once the LeNet feature detection algorithm could reliably recognise *Lomandra*

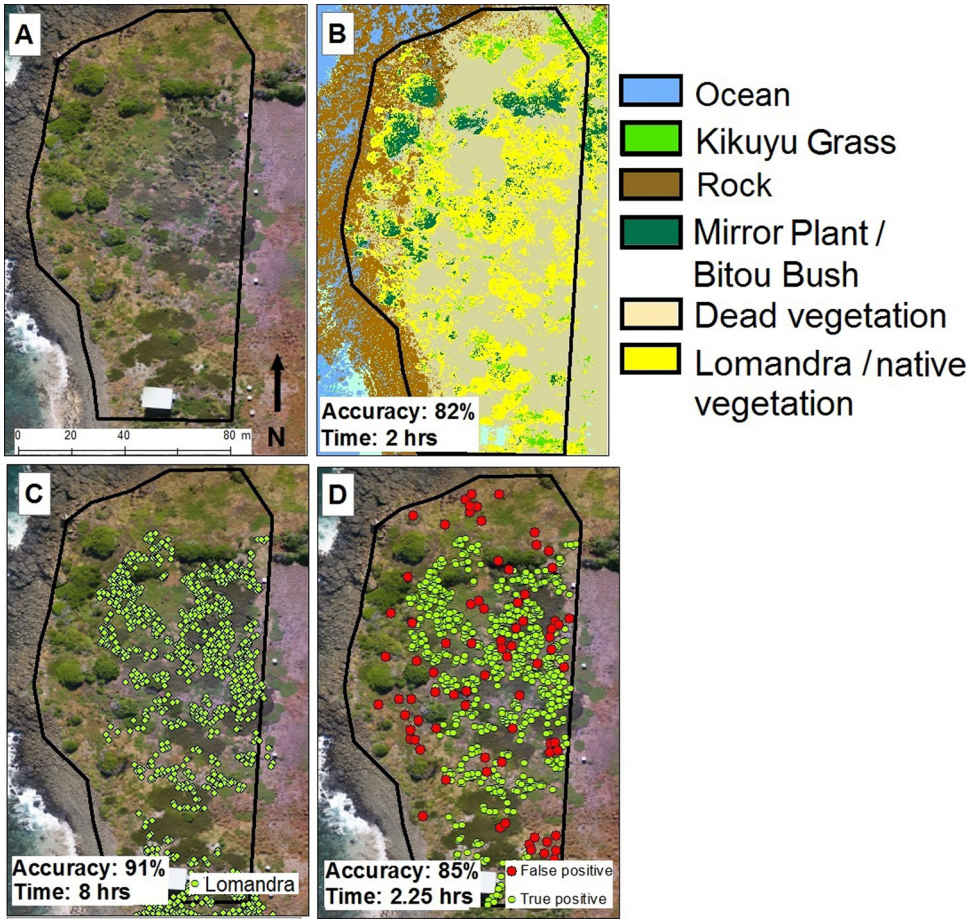

Fig. 10. A. raw UAV image mosaic for the selected weed management and planting area (May 2018), B. Pixel based classified image, C. Manually digitised *Lomandra*, D. CNN machine learning results.

tussocks on Big Island, it could do so on the remaining islands in the Five Islands Nature Reserve, or in other coastal environments. If the rehabilitation program was extended to other coastal islands of New South Wales, this mapping approach could be applied with ease.

5. Conclusions

All three approaches reliably mapped vegetation in spite of the comparably limited spectral information available in the Phantom 4 UAV images. In the case of the pixel based supervised image classification (approach 1) the cover of five different vegetation classes could

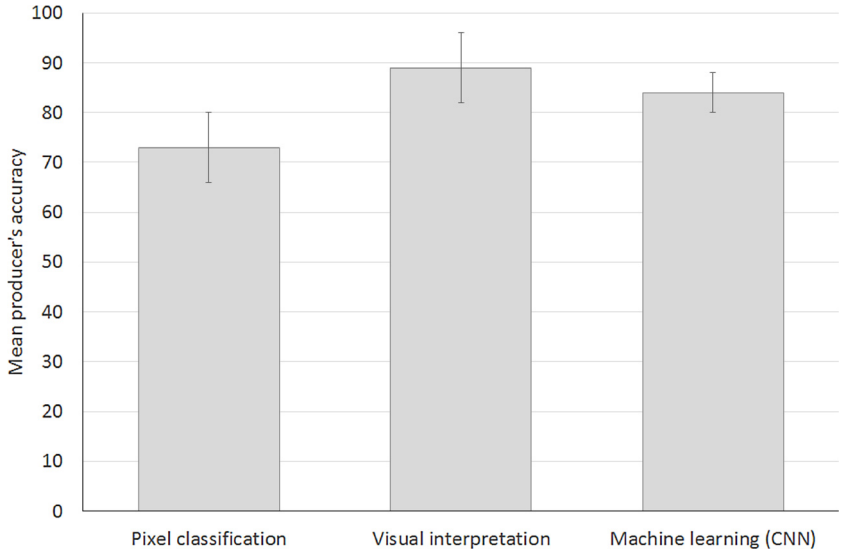

Fig. 11. Average producer's accuracy for mapping *Lomandra* plants, estimated via bootstrapping for each of the mapping approaches evaluated (twenty five calculations, 74 ground referencing points). Vertical bars indicate standard error.

reliably be discerned across the full areal extent of Big Island (Kikuyu Grass, Coastal Morning Glory, Mirror Bush, native vegetation and dead vegetation). The two maps that identified individual *Lomandra* tussocks, generated either through manual digitisation or automated detection (approaches 2 and 3, respectively) emerged as the most accurate, however, they took longer to produce. The three different mapping approaches generated fundamentally different digital information in the form of either a geographically continuous grid depicting a suite of five different vegetation community components (approach 1) or localised point datasets identifying the location of individual *Lomandra* tussocks (approaches 2 and 3). The fundamentally different nature of the vegetation maps invites greater consideration of the management objectives for which the mapping exercise is being undertaken.

The CNN machine learning algorithm established in the production of the third map emerged as a promising technique for detecting Lomandra plants as it leveraged information from both the high spatial resolution and the spatial context of the raster grids of the UAV images, while also explicitly incorporating spatial relationships within the architecture of the learning framework.

Declaration of Competing Interest

The authors declare that they have no known competing financial interests or personal relationships that could have appeared to influence the work reported in this paper.

Acknowledgements/ Funding

We are indebted to the Berrim Nuru Environmental Services of the Illawarra Local Aboriginal Land Council, staff of NSW National Parks and Wildlife Service and the Friends of Five Islands volunteers for their hard work on the vegetation regeneration program, particularly hand planting many *Lomandra longifolia* plants throughout the course of the project. UAV surveys were conducted under the National Parks and Wildlife Service Scientific Licence SL101878 with funding from the GeoQuest Research Institute (University of Wollongong). The vegetation rehabilitation project has been funded by Foundation for National Parks and Wildlife, NSW Environmental Trust Grant and the Port Kembla Community Investment Fund.

CRediT authorship contribution statement

S.M. Hamylton: Conceptualization, Data curation, Formal analysis, Funding acquisition, Investigation, Methodology, Project administration, Resources, Software, Supervision, Validation, Visualization, Writing - original draft, Writing - review & editing. **R.H. Morris:** Conceptualization, Data curation, Funding acquisition, Project administration, Writing - review & editing. **R.C. Carvalho:** Conceptualization, Data curation, Formal analysis, Writing - review & editing. **N. Roder:** Data curation, Formal analysis, Investigation, Validation, Writing - original draft. **P. Barlow:** Data curation, Formal analysis, Investigation, Validation, Writing - original draft. **K. Mills:** Supervision, Writing - review & editing. **L. Wang:** Methodology, Software, Supervision, Writing - review & editing.

Appendix A. Supplementary data

Supplementary material related to this article can be found, in the online version, at doi:https://doi.org/10.1016/j.jag.2020.102085.

References

Agisoft, L.L.C., 2014. Agisoft PhotoScan User Manual, professional edition. .

Barlow, P., 2018. A comparative study of raster and vector based approaches in vegetation mapping on Five Islands off the coast of Port kembla. School of Earth and Environmental Sciences (p. 132). University of Wollongong.

Blaschke, T., Lang, S., Hay, G., 2008. Object-based Image Analysis: Spatial Concepts for Knowledge-driven Remote Sensing Applications. Springer Science & Business Media.

Bottou, L., Vapnik, V., 1992. Local learning algorithms. Neural Comput. 4, 888–900.

Carlile, N., Lloyd, C., Morris, R., Battam, H., Smith, L., 2017. Seabird islands: big Island, Five Islands Group, New South Wales. Corella 41, 57–62.

Chenari, A., Erfanifard, Y., Dehghani, M., Pourghasemi, H., 2017. Woodland mapping at single-tree levels using object-oriented classification of unmanned aerial vehicle (UAV) images. Int. Arch. Photogramm. Remote Sens. Spatial Inf. Sci. 42.

Colefax, A.P., Butcher, P.A., Kelaher, B.P., Browman, H.E.H., 2017. The potential for unmanned aerial vehicles (UAVs) to conduct marine fauna surveys in place of manned aircraft. Ices J. Mar. Sci. 75, 1–8.

Congalton, R.G., Green, K., 2008. Assessing the Accuracy of Remotely Sensed Data: Principles and Practices. CRC press.

Davis, L.M., 1983. Notes on the Terrestrial Ecology of the Five Islands. Zoology Department, Sydney University.

Domingos, P., 2015. The Master Algorithm: How the Quest for the Ultimate Learning Machine Will Remake Our World. Basic Books.

Dujon, A.M., Schofield, G., 2019. Importance of machine learning for enhancing ecological studies using information-rich imagery. Endanger. Species Res. 39, 91–104.

Gao, J., Liao, W., Nuyttens, D., Lootens, P., Vangeyte, J., Pižurica, A., He, Y., Pieters, J.G., 2018. Fusion of pixel and object-based features for weed mapping using unmanned aerial vehicle imagery. Int. J. Appl. Earth Obs. Geoinf. 67, 43–53.

Ghazal, M., Al Khalil, Y., Hajjdiab, H., 2015. UAV-based remote sensing for vegetation cover estimation using NDVI imagery and level sets method. 2015 IEEE International Symposium on Signal Processing and Information Technology (ISSPIT) 332–337 IEEE.

Gonzalez, L., Montes, G., Puig, E., Johnson, S., Mengersen, K., Gaston, K., 2016. Unmanned aerial vehicles (UAVs) and artificial intelligence revolutionizing wildlife monitoring and conservation. Sensors 16, 97.

Hamylton, S., 2017. Spatial Analysis of Coastal Environments. Cambridge University Press.

Husson, E., Ecke, F., Reese, H., 2016. Comparison of manual mapping and automated object-based image analysis of non-submerged aquatic vegetation from very-high-resolution UAS images. Remote Sens. (Basel) 8, 724.

Krishna, K.R., 2016. Push Button Agriculture: Robotics, Drones, Satellite-guided Soil and Crop Management. Apple Academic Press.

Lawley, V., Lewis, M., Clarke, K., Ostendorf, B., 2016. Site-based and remote sensing methods for monitoring indicators of vegetation condition: an Australian review. Ecol. Indic. 60, 1273–1283.

LeCun, Y., Boser, B.E., Denker, J.S., Henderson, D., Howard, R.E., Hubbard, W.E., Jackel, L.D., 1990. Handwritten digit recognition with a back-propagation network. Advances in Neural Information Processing Systems (pp. 396-404).

LeCun, Y., Bottou, L., Bengio, Y., Haffner, P., 1998. Gradient-based learning applied to document recognition. Proc. Ieee 86, 2278–2324.

LeCun, Y., Bengio, Y., Hinton, G., 2015. Deep learning. Nature 521, 436.

Lefsky, M.A., Cohen, W.B., Parker, G.G., Harding, D.J., 2002. Lidar remote sensing for ecosystem studies: lidar, an emerging remote sensing technology that directly measures the three-dimensional distribution of plant canopies, can accurately estimate vegetation structural attributes and should be of particular interest to forest, landscape, and global ecologists. BioScience 52, 19–30.

Mather, P.M., Koch, M., 2011. Computer Processing of Remotely-sensed Images: an Introduction. John Wiley & Sons.

Matsugu, M., Mori, K., Mitari, Y., Kaneda, Y., 2003. Subject independent facial expression recognition with robust face detection using a convolutional neural network. Neural Netw. 16, 555–559.

Mills, K., 1990. Terrestrial vegetation of big Island, the Five Islands Group, port Kembla, New South Wales: 1938-1989. An historical and ecological study. Illawarra Vegetation Studies 3. Coachwood Publishing, Jamberoo, NSW June.

Mills, K., 2015. Vegetation of the Oceanic Islands of the NSW South Coast 9. Big Island, The Five Islands Group, Illawarra Coast: Exploration, exploitation and conservation. Illawarra Vegetation Studies 46. Coachwood Publishing, Jamberoo, NSW March.

Organ, M.K., Speechley, C., 1997. Illawarra Aborigines-An Introductory History.

Sandino, J., Gonzalez, F., Mengersen, K., Gaston, K.J., 2018. UAVs and machine learning revolutionising invasive grass and vegetation surveys in remote arid lands. Sensors 18, 605.

Viljanen, N., Honkavaara, E., Näsi, R., Hakala, T., Niemeläinen, O., Kaivosoja, J., 2018. A novel machine learning method for estimating biomass of grass swards using a photogrammetric canopy height model, images and vegetation indices captured by a drone. Agriculture 8, 70.

Xie, Y., Sha, Z., Yu, M., 2008. Remote sensing imagery in vegetation mapping: a review. J. Plant Ecol. 1, 9–23.

Zhu, X.X., Tuia, D., Mou, L., Xia, G.-S., Zhang, L., Xu, F., Fraundorfer, F., 2017. Deep learning in remote sensing: a comprehensive review and list of resources. Ieee Geosci. Remote. Sens. Mag. 5, 8–36.